

Postprint

This is the accepted version of a paper presented at *IEEE/RSJ International Conference on Intelligent Robots and Systems (IROS), Madrid, Spain, October 1-5, 2018.*

Citation for the original published paper:

Rudenko, A., Palmieri, L., Lilienthal, A., Arras, K. (2018)
Human Motion Prediction under Social Grouping Constraints
In: 2018 IEEE/RSJ International Conference on Intelligent Robots and Systems (IROS) (pp. 3358-3364). IEEE
https://doi.org/10.1109/IROS.2018.8594258

N.B. When citing this work, cite the original published paper.

Permanent link to this version:

http://urn.kb.se/resolve?urn=urn:nbn:se:oru:diva-71954

Human Motion Prediction Under Social Grouping Constraints

Andrey Rudenko^{1,2}, Luigi Palmieri¹, Achim J. Lilienthal² and Kai O. Arras¹.

Abstract -- Accurate long-term prediction of human motion in populated spaces is an important but difficult task for mobile robots and intelligent vehicles. What makes this task challenging is that human motion is influenced by a large variety of factors including the person's intention, the presence, attributes, actions, social relations and social norms of other surrounding agents, and the geometry and semantics of the environment. In this paper, we consider the problem of computing human motion predictions that account for such factors. We formulate the task as an MDP planning problem with stochastic policies and propose a weighted random walk algorithm in which each agent is locally influenced by social forces from other nearby agents. The novelty of this paper is that we incorporate social grouping information into the prediction process reflecting the soft formation constraints that groups typically impose to their members' motion. We show that our method makes more accurate predictions than three state-of-the-art methods in terms of probabilistic and geometrical performance metrics.

I. Introduction

Long-term prediction of human motion is an important task for applications such as robot navigation in crowded environments, autonomous driving, video surveillance or human-robot collaboration. Particularly for service robots, operating amidst humans, predicting future trajectories of surrounding people over longer periods of time has the potential to considerably enhance service quality and efficiency of human-robot interaction. Accurate, well-informed forecast of future positions of nearby humans, that goes beyond simple projection of observed velocities, allows for reasoning of the robot's global trajectory and assessing the high-level task planning more efficiently. Active anticipation of the environment's dynamics improves navigation in safety-critical scenarios, minimizing the risk of excessively reactive, overly conservative or otherwise aggressive behavior.

Making accurate predictions of future human trajectory is not a trivial task due to a number of factors. Human motion, complex and loosely constrained by nature, is furthermore influenced by the surrounding people, by the environment, its affordances and semantics, or by social rules and norms. Moreover, social and group relations among the observed people often dominate other influences on the trajectory of an individual person. Prior art has addressed this challenging task using model-based, learning-based and planning-based

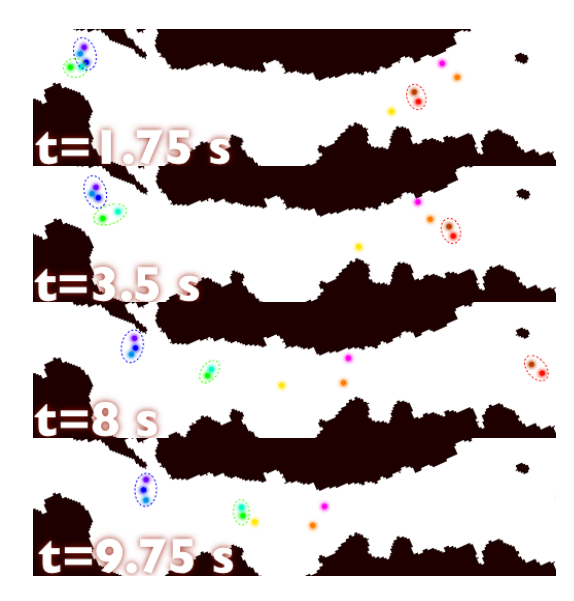


Fig. 1. Human motion in a social scenario that includes groups. Positions of several people from the ATC dataset are shown with different colors for four time instances. This part of the map includes a corridor with **black** obstacles and **white** free space. Each group is encircled with a colored line.

approaches, considering the single-agent case, ignoring other agents, or the multi-agent case, in which predictions are made jointly. However, group information is often not considered by state-of-the-art prediction algorithms.

In this paper we present a novel planning-based approach for long-term motion prediction that accounts for social interactions and grouping of the observed agents. Following our previous work [1], the presented method formulates the long-term planning problem as set of Markov Decision Processes (MDP) to produce the goal-directed global motion strategies. During online prediction, those strategies are locally modified given the soft formation constraints imposed by the group social forces [2] to account for available social information. Experiments on real-world datasets show that our method can accurately predict long-term trajectories of people involved in socially interactive tasks in real-time, outperforming three relevant state-of-the-art methods. To the best of our knowledge, this is the first attempt to bring semantic group knowledge into the long-term human motion prediction algorithm.

The paper is structured as follows: in Sec. II we discuss the related work and in Sec. III we describe our approach. Experiments and results are presented in Sec. IV and Sec. V, respectively, and Sec. VI concludes the paper.

¹A. Rudenko, L. Palmieri and K.O. Arras are with Bosch Corporate Research, Stuttgart, Germany. {andrey.rudenko, luigi.palmieri, kaioliver.arras} @de.bosch.com.

²A. Rudenko and A.J. Lilienthal are with the Center of Applied Autonomous Sensor Systems (AASS), Örebro University, Sweden. achim.lilienthal@oru.se

This work has received funding from the European Union's Horizon 2020 research and innovation programme under grant agreement No 732737 (ILIAD).

II. RELATED WORK

In the following we give a brief review of human motion prediction methods in Sec. II-A and group motion modeling approaches in Sec. II-B. We summarize the contribution of our paper in Sec. II-C.

A. Motion Prediction Approaches

Physics-based approaches [3], [4] forward-simulate a set of dynamics equations to compute pedestrian motion. To this class belongs the popular social force model [5] which is used for motion prediction by Elfring et al. [4] and in the context of tracking by Luber et al. [6].

Other common techniques for motion prediction include learning-based and planning-based methods. Learning-based methods comprise various data-driven approaches to long-term motion prediction. There are methods that learn proto-typical trajectories, "motion patterns", in a particular environment [7]. Other approaches learn typical spatial behaviors of humans navigating in social spaces [8], [9], [10]. Planning-based methods are based on the assumption that humans follow paths through the environment in an optimal, goal-directed manner. Such methods use a cost function to model navigation through the known environment [11], [1] or recover costs from observed trajectories [12].

B. Group Detection, Modeling and Prediction

Groups have a significant influence on motion of people and crowds in public spaces, such as shopping malls or airports. According to recent studies, up to 70% of people move in groups of two and more members [2], [13]. There are many methods for modeling human navigation in social scenes (e.g. the social force model [5] or cellular automaton model [14]). These models however cannot explain, realistically simulate and confidently predict human motion in social scenarios where groups are present.

The problem of formally modeling motion of people walking in groups has received increasing attention in recent years, especially for developing crowd simulation tools [15], [16], [17] and mass event planning [18], [19]. Detecting groups of people is a common task in video surveillance [20] and tracking [21], [3], [22] applications. Group detection is typically achieved through clustering of geometrically close trajectories or estimating inter- and intra-group forces among the members of the crowd. Considering group information in the motion model is known to improve the quality of people tracking [3], [22]. Common techniques for modeling group motion include imposing attraction forces to other group members [16], [22], [19], to the geometrical center of the group [2] or to the group's leader [18], or imposing a certain relative formation in which members of the group are assumed to be moving [15], [17]. An extension of the social force model that uses group information was proposed by Moussaïd et al. [2].

Methods for human motion prediction have mostly ignored group information, predicting isolated pedestrians [12], [7], [11] or considering joint predictions in a homogeneous crowd [8], [9], [10]. Existing methods for pedestrian trajectory

prediction that consider social groups usually do not assume availability of the environment's map, and model the global intention of the person simply as attraction to the goal point [22], [3]. A few methods for crowd simulation assume a better understanding of the map, e.g. using gradients indicating the most direct way towards the point of interest [19], or simply use a wave-front method to determine the shortest path to the goal [18]. These methods however operate on a per-cell basis, following certain update rules for translating the pedestrians to neighboring cells, and therefore lack the expressive representation of continuous position and velocity of agents in the social force-based models.

C. Comparison to Our Approach

In this paper we present a global planning-based approach for predicting human motion that explicitly models local collision avoidance behavior of humans. Building on our previous implementation of an MDP-based joint random walk sampling predictor [1], we augment it with the Group Social Force Model, introduced by Moussaïd et al. [2]. Unlike the learning-based techniques [7], [9], our method does not require a large training set to infer common patterns of motion behavior. It is implicitly environment-aware, does not get stuck in local minima and handles complex obstacles, contrary to physics based approaches [3], [4]. Similarly to [8], [9], [10], we jointly predict motion of multiple agents. Consideration of group information, also in the long-term perspective, is the key novelty of our approach.

III. JOINT SAMPLING MDP FOR MOTION PREDICTION

In this section we present our approach. After introducing the MDP formulation in Sec. III-A, we describe our method to generate predictions from the global motion policies in Sec. III-B with a random sampling-based algorithm, that is biased by group social forces. In Sec. III-C we analyze the complexity of our algorithm.

A. MDP For Global Motion Prediction

In this section we briefly detail the model of pedestrian's global motion towards a goal, originally presented in [1]. We use the MDP-based formulation of the optimal path planning problem in a known environment. Given a 2D static map M of the environment representing occupied and free space, and a set of goal states G, we formulate a separate MDP path finding problem for each goal $g \in \mathcal{G}$ to obtain the cost-to-go state values $V_g^*(s)$ as well as the optimal policy $\pi_{\varrho}^*(s)$ in each state $s = (s_x, s_y) \in M$. Each MDP is constructed with the absorbing zero state in the goal position. We describe actions as orientation-velocity pairs: $a = \langle \theta, \nu \rangle$, $\theta \in [0, 2\pi)$, $\nu \in [0, \nu_{\text{max}}]$. An action $a = \langle \theta, \nu \rangle$ defines the deterministic transition between states $s \xrightarrow{a} s'$, calculated as $s'_x = s_x + v \cos(\theta)$, $s'_y = s_y + v \sin(\theta)$. The reward function $\mathcal{R}_{\varrho}(s,a)$ is constructed as a weighted sum of Euclidean distance covered by a, and the unitary cost of the target state C(s'), provided by the optional input semantic map C(s).

To predict also alternative paths to the goal and allow deviations from the optimal policy, we relax the obtained π_g^* with the *stochastic Boltzmann policy* that assigns to each action a probability to be executed in state s proportional to its value $\hat{Q}_g^*(s,a)$. Temperature parameter α controls the level of stochasticity, i.e. the probability that sub-optimal actions are chosen by the agent. We denote the stochastic policy as π_g and compute it as in Eq. 1, where $\hat{Q}_g^*(s,a)$ is the value of action a, and $V_g^*(s)$ is the value of the optimal action.

$$a \sim \pi_g(s)$$
 with prob. $\propto \exp(\alpha(\hat{Q}_g^*(s, a) - V_g^*(s)))$ (1)

The obtained policy π_g allows actions up to a pre-defined very large velocity $\nu_{\rm max}$. For handling individual observed velocities $\nu_{\rm obs} < \nu_{\rm max}$, we use a simple *policy cutting* technique that incorporates information about $\nu_{\rm obs}$ into the obtained policy. For each person i, the action space is redefined with $\nu \in [0, 2\,\nu_{\rm obs}^i]$. The individual stochastic policy $\hat{\pi}_g^i$ is then computed as in Eq. 2. In $\hat{\pi}_g^i$ the probability of faster actions $a = \langle \theta, \nu \rangle$ with $\nu > \nu_{\rm obs}^i$ is set the same as for the symmetrically slower actions with $\nu < \nu_{\rm obs}^i$.

$$p(a) \text{ in } \hat{\pi}_g^i \propto \begin{cases} p(\langle \theta, \nu \rangle) \text{ in } \pi_g, \text{ if } \nu \leq \nu_{\text{obs}}^i, \\ p(\langle \theta, 2\nu_{\text{obs}}^i - \nu \rangle) \text{ in } \pi_g, \text{ if } \nu > \nu_{\text{obs}}^i \end{cases}$$
(2)

B. Joint Human Motion Prediction with Group Social Forces

In this section we present our method for jointly predicting trajectories of all agents in the scene. A people tracking system [23] is assumed to provide us short sequences of estimated positions, also called tracklets. The tracking system also estimates group information among the observed tracks by constructing a social network graph whose edges denote pairwise group relation probabilities.

Assume, there are N people in the scene. The observed track of length l(i), associated with the person i, is denoted as $\mathcal{T}^i = \langle s_1^i, s_2^i, ..., s_{l(i)}^i \rangle$, where $s_t^i = (s_{x,t}^i, s_{y,t}^i)$ is the state where the person was observed at time t, and $i \in [1, ..., N]$. The tracklet's end $s_{l(i)}^i = s^i(t_0)$ is the position of person i at the current time t_0 and \mathcal{T} is the set of all observed tracks. Membership in one and only one of the groups $Gr_h \in \mathbf{Gr}$ is assigned to each person: $i \in Gr_h$, $Gr_h \cap Gr_{h'} = \emptyset \ \forall h' \neq h$, $\bigcup_h Gr_h = \{1, ..., N\}$.

From each tracklet we derive the observed speed v_{obs}^i , orientation θ_{obs}^i and the discrete probability distribution $p^i(\mathcal{G})$ over destinations \mathcal{G} . For each goal $g \in \mathcal{G}$ we estimate the gradient of the cost-to-go $V_g^*(s)$ along \mathcal{T}^i as the difference between the costs at s_1^i and $s_{l(i)}^i$ using a softmax function:

$$p(g) \propto \exp\left(\beta\left(V_{\varrho}^{*}(s_{I(i)}^{i}) - V_{\varrho}^{*}(s_{1}^{i})\right)\right). \tag{3}$$

Temperature parameter β defines to what extent alternative goals are considered. Members of the same group Gr_h share the goal probabilities vector, computed as the average of individual vectors: $p_{Gr}^h(\mathcal{G}) = |Gr_h|^{-1} \sum_i p^i(\mathcal{G})$, $i \in Gr_h$.

1) Local Interaction and Group Motion Modeling: the social force model [5] describes how the intended motion of a person changes according to the influence the repulsive forces from other people. Formally, the social force $\mathbf{f}_{i,k}^{\text{soc}}$, emitted by person k in the direction of person i is defined as

$$\mathbf{f}_{i,k}^{\text{soc}} = a_k e^{\left(\frac{r_{i,k} - d_{i,k}}{b_k}\right)} \mathbf{n}_{i,k} \left(\lambda + (1 - \lambda) \frac{1 + \cos(\varphi_{i,k})}{2}\right), \quad (4)$$

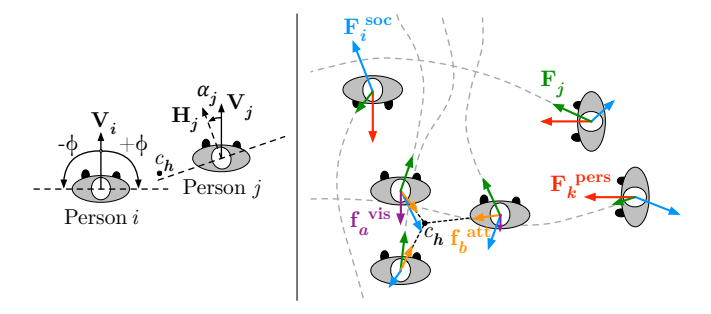


Fig. 2. Left: illustration of the group social force parameters. Right: in this example, three people a, b and c in the bottom are walking upwards as a group Gr_h . Three individual pedestrians i, j and k are opposing them from different directions. Intended directions \mathbf{F}^{pers} are shown with \mathbf{red} arrows, omitted for the group members for the sake of clarity. Person i is influenced by a strong social force \mathbf{F}^{soc} , depicted in \mathbf{blue} , and has to halt and adjust the motion trajectory, shown as a \mathbf{gray} dotted line. Person k stops and lets the group pass, while j attempts to cross in front of the group. Resulting motion directions \mathbf{F} are shown in \mathbf{green} . Intra-group social forces \mathbf{F}^{vis} and \mathbf{F}^{att} are shown in \mathbf{blue} and \mathbf{orange} respectively.

where $a_k \ge 0$ specifies the magnitude and $b_k > 0$ the range of the force, $d_{i,k}$ is the distance between people and $r_{i,k}$ is the sum of their radii. The normalized vector $\mathbf{n}_{i,k}$ pointing from k to i defines the direction of the repulsive force. An anisotropic factor $\lambda \in [0,1]$ scales the force in the person's direction of motion: the force reaches its full magnitude when the angle $\varphi_{i,k}$ between the intended motion direction of person i and $\mathbf{n}_{k,i}$ is zero, and has minimal effect when $\varphi_{i,k} = \pi$. Social forces, cast on the person i by the surrounding people, are accumulated and used to change the desired direction of motion $\mathbf{F}_i^{\text{pers}}$, which in our case is the action $a = \langle \theta, \nu \rangle$ sampled from the stochastic policy.

An extension of the social force model to include group interaction was proposed by Moussaïd et al. [2]. Several new forces are defining attraction of people walking in groups to other members of the group (attraction term) and imposing soft constraints on the walking formation that resembles typical patterns of humans in groups (visibility term). For each member i of the group Gr_h , the visibility term $\mathbf{f}_i^{\text{vis}}$ is defined as

$$\mathbf{f}_{i}^{\text{vis}} = -\beta_{1} \alpha_{i} \mathbf{V}_{i}, \tag{5}$$

where β_1 is a model parameter describing the strength of the social interaction between group members, and \mathbf{V}_i is the current velocity vector of person i. This deceleration component $\mathbf{f}_i^{\text{vis}}$ is oriented in the opposite direction of current movement \mathbf{V}_i , and it is proportional to the angle α_i between the gazing direction \mathbf{H}_i of person i and the group center of mass c_h , given the person's field of view ϕ . An illustration of the parameters is given in Fig. 2, left.

Formulation of $\mathbf{f}_i^{\text{vis}}$ imposes a *line formation*, perpendicular to the direction of motion, as the preferred walking pattern of a group. However, in order to facilitate intra-group social interactions, members of larger groups of 4 or more people often switch to the more compact *V-formation*. The same happens in cluttered spaces, as well as in crowded environments, where the members have to balance between comfortable interaction and efficient movement. To model

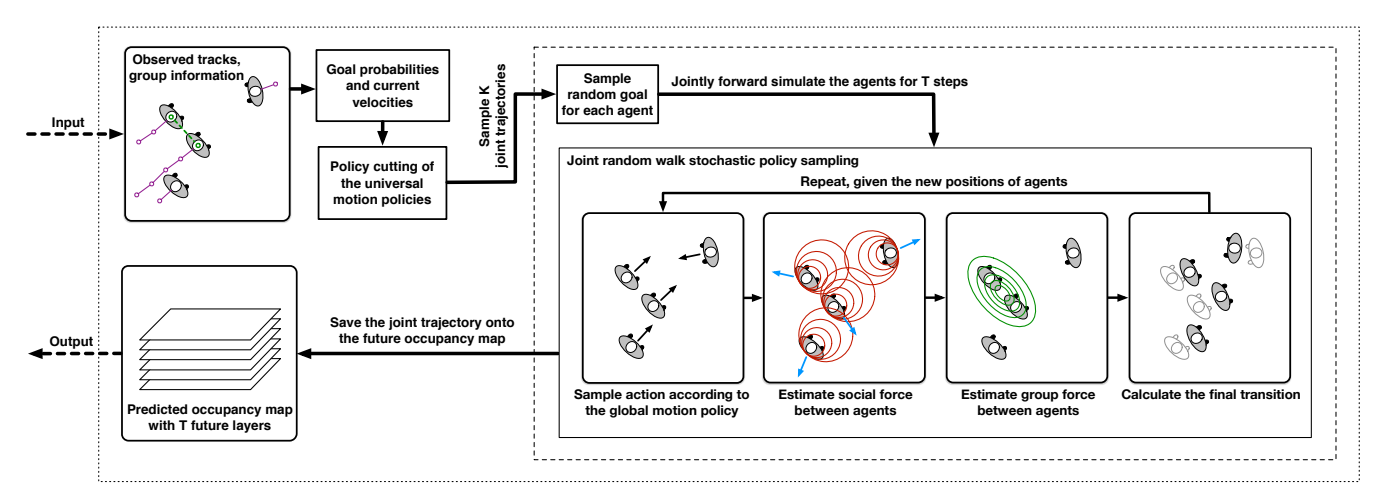


Fig. 3. Summary of the prediction workflow. Taking as input the observed tracklets and group information, out predictor samples K joint trajectories, each time drawing a random goal for the people and groups. The Joint Random Walk Stochastic Policy Sampling function estimates the social interactions and forward simulates the agents positions for T steps. Joint trajectories are then saved onto the future occupancy map.

this behavior, the attraction term $\mathbf{f}_i^{\text{att}}$ to the geometrical center of the group is introduced as

$$\mathbf{f}_{i}^{\text{att}} = \beta_2 q_A \mathbf{U}_{i},\tag{6}$$

where β_2 is the strength of the group attraction effect, and \mathbf{U}_i is the unit vector pointing from pedestrian i to the center of masses c_h of Gr_h . This force is only activated if the distance between person i and c_h exceeds a certain threshold q_A , otherwise the attraction force is zero.

The added intra-group forces $\mathbf{f}_i^{\text{vis}}$ and $\mathbf{f}_i^{\text{att}}$ yield a decelerating effect on pedestrians, whose stochastic motions often lead them in front of the group. In reality this effect is not present as humans by nature are able to better coordinate their motion within the group. To counterbalance the deceleration effect and get more precise predictions on average, we simply scale the observed speed v_{obs}^i of each human i by a factor $q_S > 1$.

The final direction of motion for person i is computed as

$$\mathbf{F}_{i} = \mathbf{F}_{i}^{\text{pers}} + \mathbf{F}_{i}^{\text{soc}} + \mathbf{F}_{i}^{\text{group}} = \mathbf{F}_{i}^{\text{pers}} + \sum_{k \neq i}^{N} \mathbf{f}_{i,k}^{\text{soc}} + \mathbf{f}_{i}^{\text{vis}} + \mathbf{f}_{i}^{\text{att}}.$$
(7)

An example of the social forces affecting the motion of people in a social scenario is given in Fig. 2, right.

2) Stochastic Policy Sampling Using Random Walks: To make predictions using the stochastic policy π_g , we utilize the random walk algorithm from our prior work [1] that samples K joint paths for all people in the scene. Each joint path is representing a possible future interaction given the observed tracklets and available social information. In each of the K samples we randomly draw a goal g(i) for person i from the distribution $p^i(\mathcal{G})$ and randomly generate actions $a^i = (\theta^i, v^i)$ from the policy corresponding to g(i). Group members share the same goal, sampled from $p^h_{Gr}(\mathcal{G})$. During the random walk, we evaluate the social interactions among the agents that affect each agent's instantaneous stochastic policy according to the group social force model. The position of each person at time t is then saved in the corresponding layer L^i_t of the probabilistic occupancy map

L, that is shared among the K samples. Each layer L_t^i is normalized to represent the probability distribution of the person's location.

The inputs of our algorithm are the map M, goals \mathcal{G} , tracklets \mathcal{T} , groups \mathbf{Gr} and the prediction horizon T. The algorithm has the following parameters: stochasticity level α , goal uncertainty β , human motion inertia coefficients I_V and I_{θ} , social force parameters $SF_p = (a_k, b_k, \lambda)$, group social force parameters $GSF_p = (\beta_1, \beta_2, q_A, \phi, q_S)$ and K joint trajectory samples. Summary of the prediction workflow is presented in Fig. 3. More information on the algorithm's parameters and implementation details is available in [1].

C. Complexity Analysis

Pseudocode in Alg. 1 summarizes the operations required to obtain predictions with our algorithm. We assume that K joint random paths are requested, N people are in the scene and T prediction steps are made. Complexity of the goal sampling operation for every human (line 2) depends on the number of goals $|\mathcal{G}|$. Group center calculation is done only once for each time step (line 4). Random action sampling procedure (line 6) depends on the action space discretization (A angles and V velocities) and has the worst-case complexity of O(AV). This happens when the agent is moving with velocity close to v_{max} . Social force in the direction of agent i (line 7) is computed for each surrounding agent within a certain radius. In the worst-case, when all agents are densely located, the complexity is O(N). Group social force computation (line 8) is a constant time operation.

Therefore, the overall complexity of our prediction algorithm is $O(K(N|\mathcal{G}|+T(N(AV+N))))$. Measurements of the runtime and comparison to the baselines are presented in Sec. V.

IV. Experiments

In this section we present several experiments conducted to evaluate qualitatively and quantitatively our *Group Social*

Algorithm 1 Joint Random Walk Stochastic Policy Sampling

```
1: for k = 1, ..., K do
2: Sample a goal for each person: O(N|\mathcal{G}|)
3: for t = 1, ..., T do
4: Calculate group center for each group: O(N)
5: for i = 1, ..., N do
6: Sample a random action: O(AV)
7: Calculate social force: O(N)
8: Calculate group social force: O(1)
```

Force MDP (GSF-MDP) approach and compare its predictive capabilities with several baselines. All algorithms are implemented in C++ and running on a laptop with a 2.8 GHz Xeon processor and 32 GB RAM. The action space of the MDP is discretized with $\pi/20$ increments of θ ; 0.1 m/s increments of ν , $\nu \in [0,3]$ m/s. Cell sizes of the grid maps are 0.05 m in Experiment 1 and 0.15 m in Experiment 2. The frequency of prediction is 4 Hz, the number of random walk samples K=200.

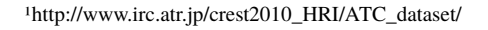
A. Experiment 1: Predicting Social Interactions

This experiment includes several qualitative demonstrations of the predicted group collision avoidance behavior of people. To this end we use define maps of two environments and simulate observed trajectories in those maps to see the predicted development of interactive scenarios. The first scenario (Fig. 4) stages an experiment with 5 people in a narrow corridor. The second scenario (Fig. 5) sets up a challenging crowded environment with multiple non-convex obstacles and 21 people walking in 7 groups.

B. Experiment 2: Prediction Evaluation

Quantitative evaluation of GSF-MDP is conducted using the ATC dataset¹ recorded in a shopping center with 15 most common goals. We extract 21 social scenarios with trajectories of 172 people, including 90 pedestrians walking in groups, observed for long periods of time (see Fig. 1 for an example scenario). Static obstacles, motion stochasticity, observation noise and extensive social interaction involving many groups makes this dataset a challenging one, particularly for methods that do not model group motion. As a baseline for predictive performance evaluation, we compare GSF-MDP to a planning-based method by Karasev et al. [11] and the social force-based approach by Elfring et al. [4]. For the sake of a fair comparison, our own goal estimation technique, that requires no training data, is applied to both baselines. Finally, we include our previous Joint Sampling MDP (JS-MDP) method from [1] in the comparison to heuristically evaluate the benefit from considering group information.

We evaluate the predictions provided by all methods based on the NLP and MHD metrics. *Negative Log-Probability* (NLP) is a probabilistic measure, that computes the average predicted probability, measured at each point i of the ground truth path \mathcal{T} for T steps into the future: $NLP(\mathcal{T}) = -\frac{1}{T}\sum_{i=1}^{T}\log\ p(\mathcal{T}_i|t_i)$. *Modified Hausdorff Distance* (MHD)



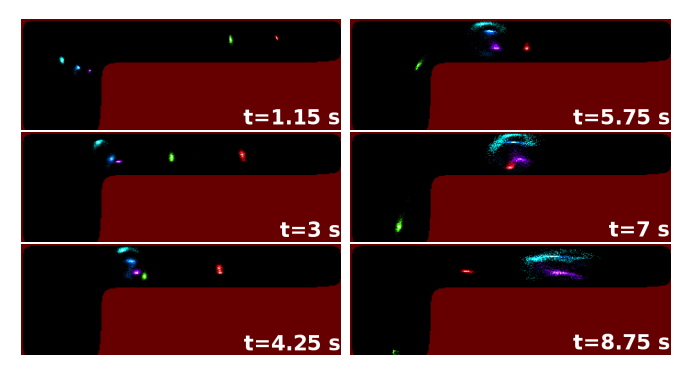


Fig. 4. Prediction results in a simulated scenario. Predicted distributions are color-coded. At t = 1.15 seconds a group of three people, depicted in **blue**, **cyan** and **purple** is walking up and then turning into a narrow corridor on the right, without losing its group formation. At t = 3, t = 4.25 seconds the group is handling a hindrance with the **green** pedestrian. At t = 5.75, t = 7 seconds the group is handling the another hindrance with the **red** pedestrian.

is a geometric measure of distance between the ground truth path and the most probable path in the predicted probability distribution. For both metrics, lower values corresponds to better prediction accuracy or smaller geometric deviation, respectively. Metric values are calculated for each trajectory in the 21 interactive scenarios and averaged across 20 experiments for each scenario. We use 1.5 seconds as observation period, and predictions are obtained for T = 2.5 - 12.5 seconds ahead. We also measure the average time to compute predictions using our algorithm and the baselines.

Prior to the main experiment, we perform hyperparameter optimization using the SMAC3 optimization toolbox [24] for each algorithm. Optimization criteria is to minimize the sum of NLP and MHD values. The optimal parameters are found to be as follows: $\alpha = 4.64$, $\beta = 18.65$, I = (0.09, 0.02), $(a_k, b_k, \lambda) = (0.09, 0.32, 0)$, $(\beta_1, \beta_2, q_A, \phi, q_S) = (0.05, 1.18, 2.93, 0.38, 1.49)$ for GSF-MDP; $\alpha = 13.26$, $\beta = 9.12$, I = (0.01, 0.19), $(a_k, b_k, \lambda) = (1.46, 0.11, 0)$ for JS-MDP; $(w_{g,t}, w_{s,t}) = (0.03, 0.14)$, $\alpha = 21.31$, $\beta = 18.68$ for [11]; $(q_w, f_w, c_w) = (1.44, 0.23, 3.1)$, $\zeta_{\rho} = 83.74$ for [4].

V. RESULTS

Fig. 4 and Fig. 5 show the results of Experiment 1. The first simulated scenario (Fig. 4) demonstrates a collision avoidance maneuver, performed by a group of three pedestrians in a narrow corridor. The group is able to keep its "social" linear walking formation that facilitates intragroup interaction. In the end, however, spreading of samples indicates the predicted possibility of re-grouping into a more compact V-formation – a behavioral pattern observed in real crowds [2]. In the second scenario (Fig. 5) our method predicts realistic behavior of group members. In particular, they are able to wait for the passage to clear before continuing their motion as a group, keeping the broad V-shape walking pattern when the available space allows it, and not lose its members behind in the dense crowd. Predicted results are visually compared with a baseline, where the group motion is not modeled.

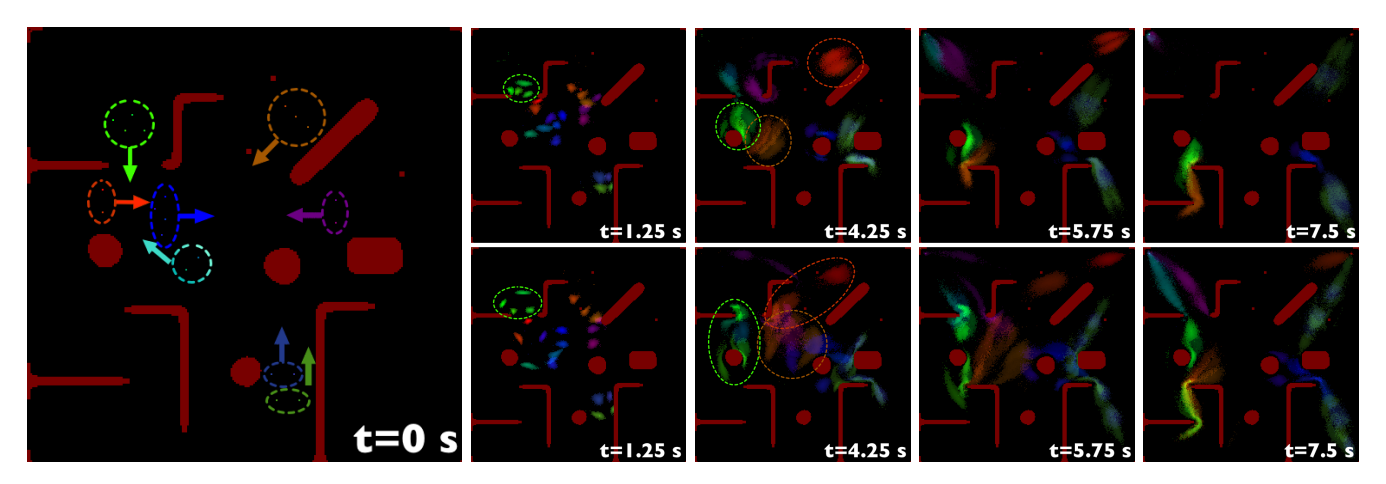


Fig. 5. Prediction results in a crowded simulated scenario with multiple obstacles and 21 people walking in 7 groups. Goals are placed in the four corners of the map. **Left:** initial positions of people are shown in colored circles, each color corresponds to one group. **Right, top row:** predicted positions with GSF-MDP for several time instances. The green group waits for the passage to clear without losing its formation. Then it gives way for the faster orange group. People in the red group are walking side by side. **Right, bottom row:** predicted positions with the JS-MDP baseline, where group motion is not modeled. The green group performs unnecessary maneuvers, then gets separated. The same happens with the red and the orange groups, who lose their members in the crowd.

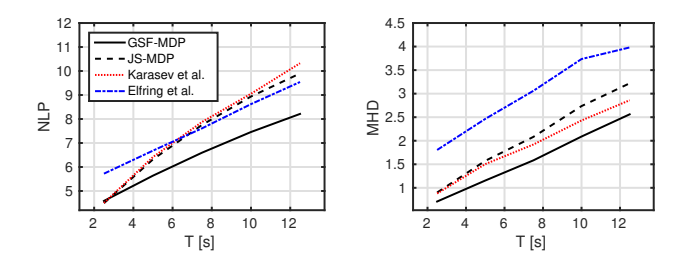


Fig. 6. **Left:** Mean of the Negative Log-Probability (NLP) metric in the ATC dataset. Our approach outperforms the baselines along the entire prediction horizon of up to 12.5 seconds. **Right:** Mean of the Modified Hausdorff Distance (MHD) metric. Our approach delivers more precise results on both short and long prediction horizons.

Fig. 6 presents the quantitative results of Experiment 2, displaying the mean of the NLP and MHD metrics over the prediction horizon of 2.5–12.5 seconds. The NLP results suggest that our algorithm assigns higher probabilities to the ground truth states of the person's future location, outperforming all the baselines. The planning-based method of Karasev et al. [11] accumulates errors from non-predicted social interactions over the growing prediction horizon, while JS-MDP [1] suffers from the lack of the group awareness. The social force-based method of Elfring et al. [4] generates worse results due to the lack of global knowledge of the environment's structure. MHD evaluation results further confirm the improvement of our method over the state-of-the-art on both short and long-term prediction horizons.

Additionally, in Fig. 7 we specify the prediction runtime of GSF-MDP, compared to the baselines. For example, our method is capable of computing 2.5 seconds of predictions for 5 people in less than 0.1 seconds, or predict 7.5 seconds of 10 people motion in 0.4 seconds. On average, our method performs on par with the state-of-the-art. Given that the range of the social force is not large, and people are not agglomerated in a single region, the method scales linearly

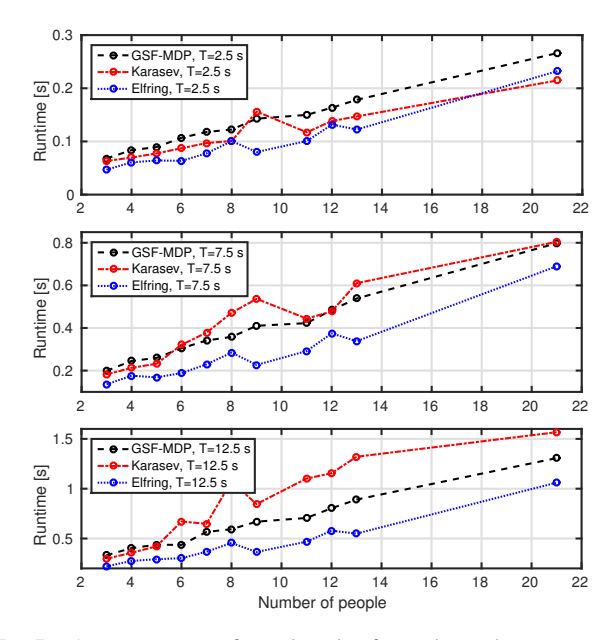


Fig. 7. Average runtime of our algorithm for prediction horizons T = 2.5, 7.5 and 12.5 seconds ahead in the ATC scenarios with various numbers of people. With respect to runtime, our method performs on par with the baselines.

with the number of people, and not quadratically as in the worst-case, described in Section III-C.

A. Discussion

The evaluation results, presented above, are encouraging. Performing at similar runtime with the state-of-the-art, our method is capable of delivering more accurate predictions. Still, during our experiments we have encountered situations, generally challenging for long-term predictors. One of them is related to overall unpredictability of human motion in the long-term perspective. A predictor should find the right uncertainty balance, similarly to precision and recall, in order

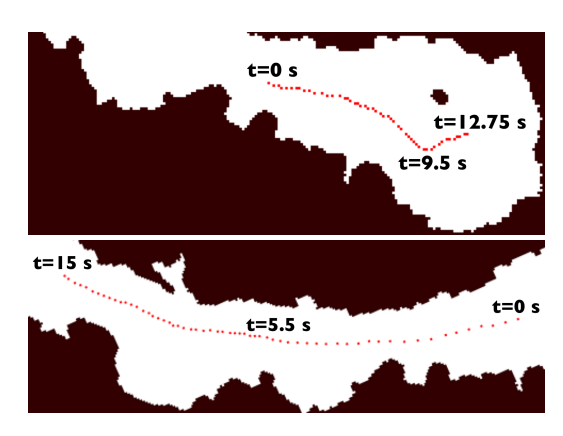


Fig. 8. Challenging observed paths from the ATC dataset. Measurements of the pedestrian's position are made at constant frequency of 4 Hz and plotted in **red**. Change of intention (**top**, at t = 9.5 seconds) and motion velocity (**bottom**, at t = 5.5 seconds) are present in these paths. In both cases there were no other people or group members nearby to explain the pedestrian's behavior.

to foresee possible unlikely events, but still stay within reasonable bounds on precision. Our stochastic policy accounts for variations in paths and homotopy classes, but does not handle sudden velocity or intention changes – this limitation in the long-term setting is a common unexplored aspect of many prediction algorithms. Predicting paths, such as in Fig. 8, is a challenging example. A possible solution may be to use a dynamic α value, which increases uncertainty for more distant points in time. Learning potential cues in the environment and incorporating them into the local behavior model is another possibility to better foresee some of the sudden intention or velocity changes.

VI. Conclusions

In this work we present a novel planning-based algorithm for predicting motion of humans, navigating in social environments. To this end we infer the long-term global intentionality by solving an MDP planning problem, and model local collision avoidance behavior of people using group social forces. We use joint sampling of the individual global motion policies by a weighted random walk process in which each person is influenced by social forces from other nearby agents and group members. Our method outperforms several baselines in terms of probabilistic and geometric measures in a real-world recorded dataset. Qualitative experiments demonstrate the ability of the method to generate realistic distributions of future motion trajectories in several interactive multi-agent scenarios. Future work will aim at more realistic, dynamic environment aware planning capabilities of predicted humans. We are also interested in comparing several group motion models, summarized in the related work section.

REFERENCES

- A. Rudenko, L. Palmieri, and K. O. Arras, "Joint prediction of human motion using a planning-based social force approach," in *IEEE Int. Conf. on Robotics and Automation (ICRA)*, 2018.
- [2] M. Moussaïd, N. Perozo, S. Garnier, D. Helbing, and G. Theraulaz, "The walking behaviour of pedestrian social groups and its impact on crowd dynamics," *PloS one*, vol. 5, no. 4, 2010.

- [3] K. Yamaguchi, A. C. Berg, L. E. Ortiz, and T. L. Berg, "Who are you with and where are you going?" in *IEEE Conference on Computer Vision and Pattern Recognition (CVPR)*, 2011.
- [4] J. Elfring, R. Van De Molengraft, and M. Steinbuch, "Learning intentions for improved human motion prediction," *Robotics and Autonomous Systems*, vol. 62, no. 4, pp. 591–602, 2014.
- [5] D. Helbing and P. Molnar, "Social force model for pedestrian dynamics," *Physical review E*, vol. 51, no. 5, p. 4282, 1995.
- [6] M. Luber, J. A. Stork, G. D. Tipaldi, and K. O. Arras, "People tracking with human motion predictions from social forces," in *IEEE International Conference on Robotics and Automation (ICRA)*, 2010.
- [7] M. Bennewitz, W. Burgard, G. Cielniak, and S. Thrun, "Learning motion patterns of people for compliant robot motion," *The International Journal of Robotics Research*, vol. 24, no. 1, 2005.
- [8] P. Trautman and A. Krause, "Unfreezing the robot: Navigation in dense, interacting crowds," in *IEEE/RSJ Int. Conf. IROS*, Oct 2010.
- [9] A. Alahi, K. Goel, V. Ramanathan, A. Robicquet, L. Fei-Fei, and S. Savarese, "Social LSTM: Human trajectory prediction in crowded spaces," in *IEEE Conf. on Computer Vision and Pattern Recognition* (CVPR), 2016.
- [10] A. Vemula, K. Mülling, and J. Oh, "Modeling cooperative navigation in dense human crowds," in *IEEE Int. Conf. ICRA*, 2017.
- [11] V. Karasev, A. Ayvaci, B. Heisele, and S. Soatto, "Intent-aware long-term prediction of pedestrian motion," in 2016 IEEE International Conference on Robotics and Automation (ICRA), May 2016.
- [12] B. D. Ziebart, N. Ratliff, G. Gallagher, C. Mertz, K. Peterson, J. A. Bagnell, M. Hebert, A. K. Dey, and S. Srinivasa, "Planning-based prediction for pedestrians," in *IEEE/RSJ International Conference on Intelligent Robots and Systems*, Piscataway, NJ, USA, 2009.
- [13] L. Cheng, R. Yarlagadda, C. Fookes, and P. K. Yarlagadda, "A review of pedestrian group dynamics and methodologies in modelling pedestrian group behaviours," World, vol. 1, no. 1, pp. 002–013, 2014.
- [14] C. Burstedde, K. Klauck, A. Schadschneider, and J. Zittartz, "Simulation of pedestrian dynamics using a two-dimensional cellular automaton," *Physica A: Statistical Mechanics and its Applications*, 2001.
- [15] I. Karamouzas and M. Overmars, "Simulating and evaluating the local behavior of small pedestrian groups," *IEEE Transactions on Visualization and Computer Graphics*, vol. 18, no. 3, 2012.
- [16] F. Qiu and X. Hu, "Modeling group structures in pedestrian crowd simulation," Simulation Modelling Practice and Theory, 2010.
- [17] H. Singh, R. Arter, L. Dodd, P. Langston, E. Lester, and J. Drury, "Modelling subgroup behaviour in crowd dynamics dem simulation," *Applied Mathematical Modelling*, vol. 33, no. 12, 2009.
- [18] M. Seitz, G. Köster, and A. Pfaffinger, "Pedestrian group behavior in a cellular automaton," in *Pedestrian and Evacuation Dynamics*, 2012.
- [19] S. Bandini, F. Rubagotti, G. Vizzari, and K. Shimura, "An agent model of pedestrian and group dynamics: experiments on group cohesion," AI* IA 2011: Artificial Intelligence Around Man and Beyond, 2011.
- [20] J. Šochman and D. C. Hogg, "Who knows who-inverting the social force model for finding groups," in *IEEE International Conference on Computer Vision Workshops (ICCV Workshops)*, 2011.
- [21] T. Linder and K. O. Arras, "Multi-model hypothesis tracking of groups of people in rgb-d data," in *Information Fusion (FUSION)*, 2014 17th International Conference on. IEEE, 2014, pp. 1–7.
- [22] S. Pellegrini, A. Ess, and L. Van Gool, "Improving data association by joint modeling of pedestrian trajectories and groupings," in *European Conference on Computer Vision*. Springer, 2010, pp. 452–465.
- [23] T. Linder, S. Breuers, B. Leibe, and K. O. Arras, "On multi-modal people tracking from mobile platforms in very crowded and dynamic environments," in *IEEE Int. Conf. on Robotics and Automation*, 2016.
- [24] M. Lindauer, K. Eggensperger, M. Feurer, S. Falkner, A. Biedenkapp, and F. Hutter, "Smac v3: Algorithm configuration in python," https://github.com/automl/SMAC3, 2017.
- [25] S. Koenig and M. Likhachev, "D*lite," in 18th National Conference on Artificial Intelligence. AAAI, 2002.